



Abstract Reviewed Paper at ICSA 2019

Presented * by VDT.

Detection of Constant Phase Shifts in Filters for Sound Field Synthesis

Frank Schultz, Nara Hahn, and Sascha Spors

University of Rostock, Institute of Communications Engineering

Email: {frank.schultz, nara.hahn, sascha.spors@uni-rostock.de}

Abstract

Filters with constant phase shift in conjunction with 3/6 dB amplitude decay per octave frequently occur in sound field synthesis and sound reinforcement applications. These ideal filters, known as (half) differentiators, exhibit zero group delay and 45/90 degree phase shift. It is well known that certain group delay distortions in electro-acoustic systems are audible for trained listeners and critical audio stimuli, such as transient, impulse-like and square wave signals. It is of interest if linear distortion by a constant phase shift is audible as well. For that, we conducted a series of ABX listening tests, diotically presenting non-phase shifted references against their treatments with different phase shifts. The experiments revealed that for the critical square waves, this can be clearly detected, which generally depends on the amount of constant phase. Here, -90 degree (Hilbert transform) is comparably easier to detect than other phase shifts. For castanets, lowpass filtered pink-noise and percussion the detection rate tends to guessing for most listeners, although trained listeners were able to discriminate treatments in the first two cases based on changed pitch, attack and roughness cues. Our results motivate to apply constant phase shift filters to ensure that also the most critical signals are technically reproduced as best as possible. In the paper, we furthermore give analytical expressions for discrete-time infinite impulse response of an arbitrary constant phase shifter and for practical filter design.

1. Introduction

Sound reproduction systems for large audiences are often equipped with vertical loudspeaker arrays which shall deliver an equally pleasant acoustic experience to the audience in terms of loudness, timbre and spatial impression. The reproduced wavefront can be steered and shaped towards the target region by applying delays and weights to the individual loudspeaker signals [1, 2]. Due to the coherence of these, the sound field typically exhibits a low-pass filter characteristic, and thus needs to be equalized by high-pass filtering the audio input signal. As pointed out in [3, Ch. 3], the same array processing framework is used in wave field synthesis (WFS), which has only seemingly a different goal, namely the physical reconstruction of a desired sound field. The loudspeaker signals for WFS are derived from a high-frequency approximation of the Kirchhoff-Helmholtz integral

equation [4, 5]. This enables a computationally efficient implementation of WFS which comprises of, similar to large-scale sound reproduction, delays and weights for the individual loudspeakers and an overall equalization filter.

According to the theory of WFS [4], the specification of the equalization filter depends on the geometry and shape of the loudspeaker array. The transfer function is $i\omega$ for 3D scenarios where 2D arrays (e.g. spherical or planar) are used. In terms of signals and systems theory this constitutes an differentiator, exhibiting a slope of +6 dB per octave and a constant phase of 90°. For 2D scenarios using 1D arrays (e.g. circular and linear), the filter is given as $\sqrt{i\omega}$, constituting a half-differentiator [6, 7], where both the slope and phase are halved to +3 dB per octave and 45°, respectively.

In practical systems, where a continuous and infinite array cannot be used, the specification of the equalization filter has to be adjusted accordingly. The usage of a practical array

built from individual loudspeakers causes spectral fluctuations above the so-called spatial aliasing frequency [4]. Moreover, due to the finite extent of the array, the synthesized sound field exhibits a low frequency roll off. The high-pass filter characteristic of an ideal equalization filter thus should be flattened out at the highest and lowest frequencies in the spectrum, resulting in a high-pass shelving filter. The upper limit coincides with the spatial aliasing frequency and the lower limit is determined by the spatial extent of the array [8].

The digital equalization filter is typically realized either in a finite impulse response (FIR) or infinite impulse response (IIR) form. FIR type equalization filters are often designed as linear phase, while omitting the above mentioned constant phase (90° or 45°) [9, 10]. This results in synthesized sound fields exhibiting a negative phase shift (-90° or -45°) compared to the desired reference sound field (apart from the group delay of the FIR filter). There are also a number of IIR type equalization filters where the constant phase spectrum is explicitly taken into account [11] or comes as a byproduct of the minimum phase characteristics of the desired magnitude spectrum [3, 12]. The improved physical accuracy in the synthesized sound field is well demonstrated in [12, Fig. 9–11].

The audibility of constant phase shifts can be regarded as special issue of the audibility of phase distortion and group delay distortion, cf. [13–18], often evaluated with allpass filters. From these works it is known, that audibility is strongly dependent of the signal’s waveform and spectrum and the amount of the group delay in the critical bands. Generally, sensitivity for phase/group delay distortions decreases with increasing frequency. For low frequency content a different pitch and for high frequency content ringing and different lateralization is reported for group delay distortions. The polarity of highly transient signals plays a role for the audibility. It was often shown, that training on phase/group delay distorted audio content increases the sensitivity to detect them.

To the authors’ knowledge to date, the perceptual impact of the constant phase shift has not been studied yet. It is of great interest whether the existence or absence of such a phase shift is audible, and in the special context of sound field synthesis, if this affects the authenticity of the synthesized sound fields. The paper discusses the signal processing fundamentals of discrete-time constant phase shift in Sec. II. In Sec. III a listening test is presented for selected audio content and phase shifts to initially evaluate the audibility of constant phase shifts. Sec. IV concludes the paper.

2. Constant Phase Shifter

A constant phase shifter, also known as fractional Hilbert transformer [19], refers to a filter that applies a (frequency independent) constant shift φ to the spectrum of an input signal. This section introduces the time and frequency representations of discrete-time constant phase shifters for aperiodic and periodic signals. Practical implementations for the respective cases are also discussed. Since the primary interest of the present study is the audibility of a phase shift, the main consideration is the accuracy of the constant phase shifter in terms of its magnitude and phase response. Computational

cost and algorithm optimization are less of a concern.

2.1. Aperiodic Signals

The transfer function of a constant phase shifter in the discrete time Fourier transform (DTFT) domain reads

$$H(e^{i\Omega}) = \begin{cases} e^{+i\varphi}, & 0 < \Omega < \pi \\ e^{-i\varphi}, & -\pi < \Omega < 0 \\ \cos \varphi, & \Omega = 0, \pi \end{cases} \quad (1)$$

where $\Omega = \frac{2\pi f}{f_s}$ denotes the normalized angular frequency for the sampling rate f_s . By exploiting Euler’s formula, (1) can be decomposed into

$$H(e^{i\Omega}) = \cos \varphi - \sin \varphi \cdot H_H(e^{i\Omega}), \quad (2)$$

with $H_H(e^{i\Omega}) := -i \cdot \text{sgn}_\Omega$ denoting the transfer function of the Hilbert transformer [20]. Notice that the Hilbert transformer can be regarded as a constant phase shifter of $\varphi = -\frac{\pi}{2}$. Since $H_H(e^{i\Omega})$ is free of DC bias [20, Sec. 4.2], the magnitude response of a constant phase shifter is unity at all frequencies but $\Omega = 0, \pi$, as given in (1).

The discrete-time impulse response of a constant phase shifter is obtained by computing the inverse DTFT of $H(e^{i\Omega})$,

$$h[n] = \begin{cases} \cos \varphi, & n = 0 \\ 0, & n \neq 0 \text{ and even} \\ -\frac{2}{n\pi} \sin \varphi, & n \text{ odd.} \end{cases} \quad (3)$$

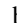

Analogous to (2), it comprises of two components,

$$h[n] = \cos \varphi \cdot \delta[n] - \sin \varphi \cdot h_H[n] \quad (4)$$

where

$$h_H[n] = \begin{cases} 0, & n \text{ even} \\ \frac{2}{n\pi}, & n \text{ odd.} \end{cases} \quad (5)$$

denotes the discrete-time impulse response of the Hilbert transform filter [21, Eq. (11.65)]. The constant phase shift of an input signal is thus a linear combination of the input itself and its Hilbert transform, weighted with $\cos \varphi$ and $-\sin \varphi$, respectively.

In Fig. 1(left), the impulse response $h[n]$ for $\varphi = -\frac{\pi}{4}$ is depicted. It can be seen that the impulse response is of infinite length and not causal. The coefficients for $n \neq 0$, indicated by , exhibit odd symmetry with respect to $n = 0$ and add up to 0. The DC and $\frac{f_s}{2}$ gain are thus solely determined by $h[0] = \cos \varphi$, indicated by  and consistently given in (1).

Filtering with the impulse response $h[n]$ is not feasible in practice due to the infinite extent of $h[n]$. An FIR constant phase shifter can be built by applying a finite window to $h[n]$, known as windowing method [21, Sec. 7.2]. Considering the decay of the coefficients for $|n| \rightarrow \infty$, it is a natural choice to truncate the impulse response symmetrically with respect to $n = 0$, which leads to an even-order (odd-length) FIR filter. Since $h[n]$ vanishes for even $n \neq 0$, the FIR length N has to satisfy $N \bmod 4 = 3$ (i.e. $N = 3, 7, 11, 13, \dots$). Using a tapering window is advantageous as it smooths out the

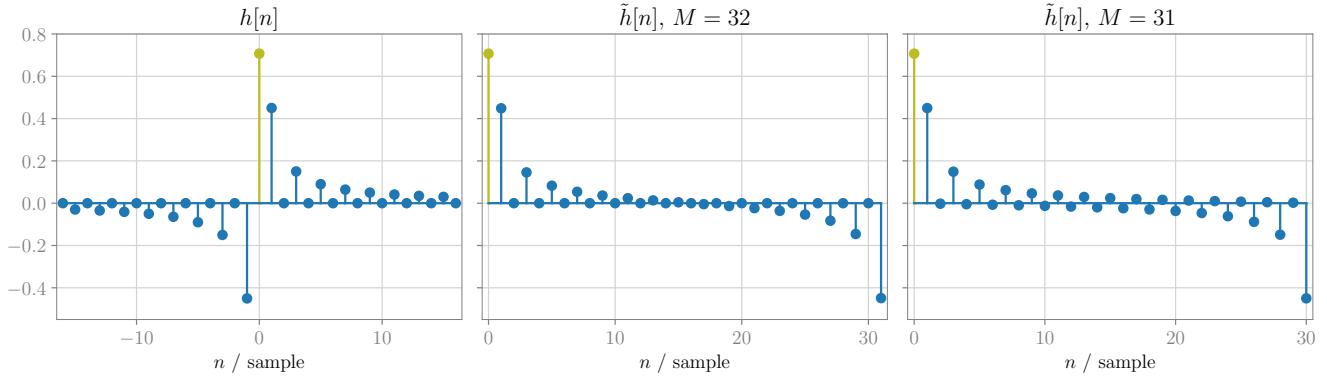


Fig. 1: Left: Impulse response of a constant phase shifter ($\varphi = -45^\circ$) described in (3). Center & Right: Impulse responses of periodic constant phase shifter ($\varphi = -45^\circ$) for even and odd period M , described in (8) and (9), respectively. The coefficients $h[0] = \tilde{h}[0] = \cos \varphi$ are indicated by \blacktriangledown . The coefficients for $n \neq 0$ indicated by \blacktriangledown show the Hilbert transform part of the impulse response.

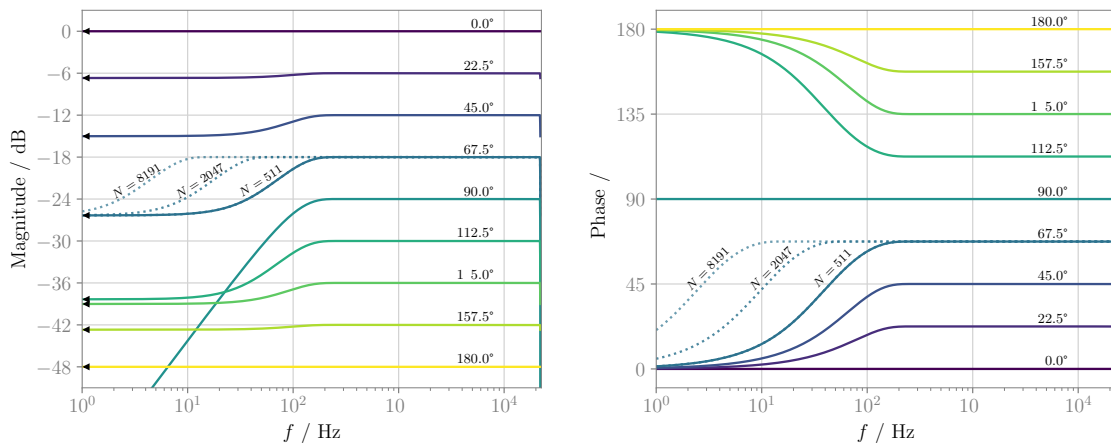


Fig. 2: Frequency responses of constant phase shifters (left: magnitude, right: phase, $f_s = 44.1$ kHz). The FIR filter coefficients are obtained by using the windowing method (filter length of $N = 511$ for all angles and $N = 511, 2047, 8191$ for $\varphi = 67.5^\circ$). The magnitude responses are depicted with 6 dB offsets. The triangles \blacktriangleleft indicate the DC gain $\cos \varphi$. The phase responses are obtained by compensating the group delay $\tau = \frac{N-1}{2} \frac{1}{f_s}$, i.e. multiplying the complex exponential $e^{i2\pi f \tau}$ to the spectra.

ripples in the frequency domain. Due to the non-causality of the filter, a constant group delay of $\tau = \frac{N-1}{2} \frac{1}{f_s}$ is introduced additionally to the desired property given by (1).

Exemplary frequency responses of FIR constant phase shifters ($\varphi = 0^\circ, \dots, 180^\circ$) are shown in Fig. 2. The FIR coefficients are obtained by applying a Blackman window to $h[n]$ in (3). It can be seen that the desired magnitude and phase responses are achieved only within a limited frequency band. For $\varphi \neq 0^\circ, 180^\circ$, the magnitude responses typically attenuate at low and high ends ($f = 0$ and $f = \frac{f_s}{2}$, respectively) and converge to $\cos \varphi$. Due to the logarithmic frequency axis, the behavior at $f = \frac{f_s}{2}$ is not clearly visible, though. For $\varphi \neq 90^\circ$, the phase responses are inaccurate at both ends and gradually tend to 0° or 180° . The constant phase shifter for $\varphi = 90^\circ$ exhibits an ideal phase response but the most distorted magnitude response among other phase angles. Accurate frequency responses are observed for $\varphi = 0^\circ, 180^\circ$ where the filters are integer delays ($\tau = \frac{N-1}{2} \frac{1}{f_s}$) with non-inverted and inverted polarity. As indicated by dotted lines ($\varphi = 67.5^\circ$) in Fig. 2, the spectral distortions can be suppressed by increasing the FIR filter order, which comes at the expense of an increased group delay.

2.2. Periodic Signals¹

Consider an M -periodic signal $\tilde{s}[n] = \tilde{s}[n + M]$ and the generating signal $s[n]$ which coincides with $\tilde{s}[n]$ for the period $n = 0, \dots, M-1$ and vanishes elsewhere. Then the periodic signal can be represented as a shifted sum of $s[n]$,

$$\tilde{s}[n] = \sum_{\mu=-\infty}^{\infty} s[n] * \delta[n - \mu M], \quad (6)$$

where $*_n$ denotes the linear convolution with regard to n . The constant phase shift of $\tilde{s}[n]$ reads

$$\tilde{y}[n] = \tilde{s}[n] * h[n] = s[n] * \underbrace{\sum_{\mu=-\infty}^{\infty} h[n - \mu M]}_{\tilde{h}[n]}, \quad (7)$$

meaning that the generating function $s[n]$ is convolved with an infinite sum of shifted impulse responses denoted by $\tilde{h}[n]$. A closed form expression for $\tilde{h}[n]$ can be obtained by

¹The derivation in this subsection is adopted from [20, Sec. 1.9 and Sec. 4.6].

substituting (4) for $h[n]$ and exploiting the series expansion of the cotangent function [22, Eq. (4.3.91)], reading

$$\tilde{h}[n] = \begin{cases} \cos \varphi, & n = 0 \\ 0, & n \neq 0 \text{ and even} \\ -\frac{2 \sin \varphi}{M} \cot\left(\frac{\pi n}{M}\right), & n \text{ odd,} \end{cases} \quad (8)$$

for even M , and

$$\tilde{h}[n] = \begin{cases} \cos \varphi, & n = 0 \\ -\frac{\sin \varphi}{M} \cot\left(\frac{\pi(n+M)}{2M}\right), & n \neq 0 \text{ and even} \\ -\frac{\sin \varphi}{M} \cot\left(\frac{\pi n}{2M}\right), & n \text{ odd,} \end{cases} \quad (9)$$

for odd M . Exemplary impulse responses are shown in Fig. 1(center, right) for $\varphi = -45^\circ$.

A periodic repetition of a signal in the time domain is equivalent to a sampling of the spectrum in the DTFT domain [21, Sec. 8.4]. The discretized DTFT spectrum then constitutes the discrete Fourier transform (DFT) spectrum [21, Sec. 8.5], for which periodicity of the signal and the spectrum are inherent. The DFT coefficients for even M read

$$H[k] = H(e^{i\frac{2\pi}{M}k}) \quad (10)$$

$$= \begin{cases} e^{+i\varphi}, & k = 1, \dots, \frac{M}{2} - 1 \\ e^{-i\varphi}, & k = \frac{M}{2} + 1, \dots, M - 1 \\ \cos \varphi, & k = 0, \frac{M}{2} \end{cases}$$

where $H[k]$ denotes the DFT of $\tilde{h}[n]$. Note that (8), (9), and (10) are analytic representations of the constant phase shifter with no approximations involved. An ideal constant phase shift is therefore feasible as far as periodic discrete-time signals are concerned.

In practice, a constant phase shift of a periodic signal can be computed efficiently in the DFT domain,

$$y[n] = \frac{1}{M} \sum_{k=0}^{M-1} S[k] H[k] e^{i\frac{2\pi}{M}kn}, \quad (11)$$

for $n = 0, \dots, M - 1$, where $S[k]$ denotes the DFT of $s[n]$. This constitutes a circular convolution of $s[n]$ and $\tilde{h}[n]$, and $y[n]$ exhibits a temporal aliasing which constitutes the desired result, as shown in (7). Finally, the periodic signal $\tilde{y}[n]$ is constructed with the generating signal $y[n]$, in the same way as (6).

3. Listening Experiment

We aim at investigating, if audio content treated with a constant phase shift filter can be perceptually discriminated from the original signals. This section discusses the design, procedure and analysis of the conducted listening experiment, related to this question.

3.1. ABX Test Framework

The discrimination performance was tested with the highly sensitive two alternatives, forced choice ABX test. Stimuli A and X were both randomly assigned to either the reference (original) or the treatment (phase shift), subsequently ensuring

that B contains the other stimulus than A. According to the ABX test paradigm, test subjects were asked to assign either X=A or X=B after thorough, non-time-limited comparison of A, B and X.

No looped playback or instantaneous stimulus switching with crossfade or fast fade-out/fade-in could be utilized, since treatment detection would have become a trivial task based on the resulting artifacts (i.e. clicks for fade-out/in, phasing for crossfade). Instead, the stimuli—always (re)-started from the beginning—had to be manually started and stopped by the test subjects. This ensures artifact free playback, although with higher interaction. Moreover, the requirements led to some modifications of the utilized webMUSHRA test framework [23], which by default intends seamless switching and looping by fading out/in.

3.2. Audio Content

The 4 monaural audio contents

- three square wave burst signals, each: 50 Hz, 200 ms on including 40 ms \sin^2 -fade in and out, 300 ms off. Fourier series synthesis of the harmonics 1, 3, ..., 19, modal windowing (Kaiser, $\beta = 4$) of the Fourier coefficients. total length 1.5 s @ 120 bpm, periodicity assumed / DFT filtering
- pink noise², lowpass filtered (4th order Butterworth, cut frequency 300 Hz), length 2.35 s, non-periodicity assumed / FIR filtering
- castanets³, length 2 s, periodicity assumed / DFT filtering
- Hotel California, Eagles, Hell freezes over, 1994, Geffen, stereo version mixdown to mono, time range 0:44.938 - 0:48.142, non-periodicity assumed / FIR filtering

were chosen to create the 5 treatments

- I square wave burst with $\varphi = -90^\circ$
- II square wave burst with $\varphi = -45^\circ$
- III lowpass filtered pink noise with $\varphi = -90^\circ$
- IV castanets with $\varphi = -90^\circ$
- V Hotel California with $\varphi = -90^\circ$,

according to the following considerations: It is known that human hearing is sensitive to group delay variations of low frequency square wave bursts [16], which is assumed to hold for constant phase shifts as well. To evaluate a potential detection of phase shifts for highly transient audio material and to check for potential detection of pre-/postringing due to filtering of such, castanets were included. Phase alignment in noise signals is highly random. It was assumed that human hearing is sensitive to a varied phase structure of noise with a low frequency spectrum. Furthermore, a musical record with a percussion sequence—commonly considered as very high fidelity production (mixing: E. Scheiner, mastering: T.

²generated by Voss-McCartney algorithm:
<https://github.com/AllenDowney/ThinkDSP/blob/master/code/voss.ipynb>

³anechoic version of EBU SQAM CD track 27:
<https://iaem.at/Members/frank/sounds/castanets-dry>

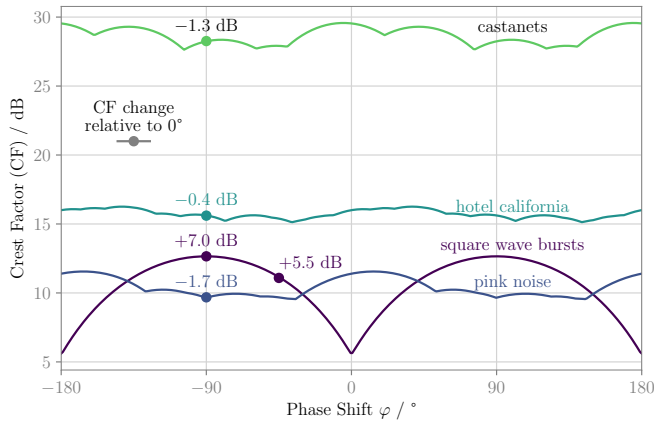


Fig. 3: Crest factor over phase shift for the 4 audio contents used in the listening test.

Jensen)—was included. For that content, it was assumed that a constant phase shift might be audible in the decay of the drumheads or/and in the transients.

For the treatments I, II and IV signal periodicity is assumed and thus the ideal phase shift filter via DFT (Sec. 2.2) was applied. To create treatments V and III, no signal periodicity was assumed for the whole musical piece as well as for the generated pink noise raw material of 6 minutes duration. Thus FIR filtering according to Sec. 2.1 was realized. Considering the audio contents as rectangularly windowed signals of infinite duration, the filter order of 3963530 (≈ 90 s!) ensures that linear convolution of the chosen excerpt of Hotel California is complete. The resulting magnitude ripple of the Blackman windowed FIR is negligible for the relevant reproduction bandwidth. Since the pink noise length can be arbitrarily set, the same FIR filter was utilized for consistence.

3.2.1. Crest Factor Discussion

An ideal constant phase shifter does not alter the spectrum of the input signal, nor does it introduce any group delay. One noticeable technical change concerns the waveform, quantifiable in terms of the crest factor (CF),

$$CF = 20 \log_{10} \left(\frac{|s|_{\text{PEAK}}}{s_{\text{RMS}}} \right) \text{ in dB.} \quad (12)$$

During the preparation of this study, it was speculated that an increase or decrease of the CF might lead to detectable cues (if there are any) for a phase shift.

Figure 3 depicts the CF of the chosen audio contents for varying phase shifts $\varphi \in [-180^\circ, 180^\circ]$. For aperiodic signals (pink noise and Hotel California), the phase shift is applied to the entire piece but the CF is evaluated only for the selected part which is used in the listening experiment. Notice that the CF is 180° -periodic. This is because a phase shift of 180° reverses the polarity of the signal and the CF remains unchanged. Among other stimuli, the square wave burst shows the highest variation of approximately 7 dB. Note, however, that due to the silence between the bursts and the temporal shaping by the fade-in/-out window, the CF deviates from that of a continuous square wave (which is theoretically

$CF = 0$ dB for $\varphi = 0^\circ, \pm 180^\circ$ and $CF = \infty$ for $\varphi = \pm 90^\circ$). The CF of castanets is about 15 to 25 dB higher than other stimuli because of its fast attack/decay, very short sustain, and relatively long silence.

As mentioned in Sec. 1, phase angles of -90° and -45° are particularly of our interest due to the relation with the equalization filter in WFS. Except for square waves, a phase shift of -45° is barely detectable for most of the audio materials that was tested in informal listening. Therefore, -90° is predominantly tested in this study whereas -45° is included only for square wave bursts. In Fig. 3, the CF change of the phase shifted stimuli relative to the original signal ($\varphi = 0^\circ$) is annotated above the filled circles \bullet .

3.2.2. Audio Signal Processing and Rendering

Each reference audio content (except castanets) was loudness calibrated to -23 LUFS [24]. The according calibration gain was also applied to the associated phase shifted stimuli. Since the loudness measure of [24] is suboptimal for castanets, perceptually motivated re-calibration to -35 LUFS was pursued in order to better match playback level with the other audio contents. Non-dithered 24 Bit, 44.1 kHz PCM wav-files were rendered for all required stimuli, carefully monitoring that amplitude clipping—as undesired artifact blended with the phase shift—does not occur.

3.3. ABX Test Statistics Considerations

All test subjects were to rate the 5 different treatments created from the 4 audio contents in mixed, randomized order and—except for the two lead authors—without preliminary training or other preconditioning with respect to the research question.

For each of the 5 treatments 25 ABX trials had to be rated, resulting in $5 \cdot 25 = 125$ judgments per test subject aiming at evaluation of individual detection rates in the first instance. Thus, with underlying Binomial distribution model [25, 26], these quantities originate from intended one-side tail hypothesis testing of the $\mathcal{H}_0(p_{\text{detect}} = 0.5)$ using Bonferroni correction to a target rejection level $\alpha = 0.05$, a target test power $1 - \beta = 0.95$ and an effect size of $g = 0.4$, which was determined from preliminary test results using square wave bursts, achieving detection probabilities of about $p_{\text{detect}} = 0.9$.

Assuming independence of all collected ratings, contingency tables of detection frequencies can be statistically evaluated with underlying Chi-Square (χ^2) distribution model as post hoc tests.

3.4. Experiment Procedure

The listening test was conducted in our loudspeaker array lab with 0.3 s mean RT60 and about 40 dB(A)_{Leq} sound pressure level (SPL) of background noise. A large monitor, a keyboard and a mouse were set up on a table, where test subjects took seat in the middle of the lab during the experiment. The browser based ABX GUI of the webMUSHRA software was hosted on an Apple Mac Mini connected to an RME Fireface UC.

Playback was presented diotic (i.e. same signal for both ears) using an electrodynamic, circumaural, open headphone Sennheiser HD 800. Playback level was settled such that for a mono pink noise signal with -23 LUFS loudness

($-7.8 \text{ dB}_{\text{TruePeak}}$, $-21.3 \text{ dB}_{\text{RMS}}$, i.e. $13.5 \text{ dB}_{\text{CF}}$) sound pressure levels (SPLs) of $72.7 \text{ dB(A)}_{\text{Leq}} / 87.7 \text{ dB(C)}_{\text{Peak}}$ were measured for the left and the right channel using a G.R.A.S. headphone-to-ear coupler and a calibrated Brüel & Kjaer SPL meter according to the IEC 60318 standard.

12 test subjects (4 female, 8 male) took part in the listening experiment. Except one light tinnitus afflicted, all others reported normal hearing. Test subjects' age distribution is given as $\mu_a = 29.8$, $\sigma_a = 6.5$ years with the percentiles $a_{0.05} = 22.6$, $a_{0.25} = 25$, $a_{0.5} = 28$, $a_{0.75} = 32$, $a_{0.95} = 40.5$ years. About half of the listening test panel consists of music production experts and (future) professional musicians (classical instrument students). The other half recruits from research related, untrained listeners, occasionally without prior experience in performing listening tests.

For familiarization of the specific ABX GUI, ratings on full band pink noise with 1 dB level difference were performed by each test subject prior to the actual listening test. This procedure was accompanied by written operational instructions and remarks, indicating that the differences to be detected in the actual listening test might be very subtle and will potentially differ in character compared to that of the training session. Participants (except the two authors) were left completely uninformed with respect to the signal manipulation method, thus expecting unbiased strategies for the detection of differences.

After many pre-listening experiments, we decided against playback of all 25 trials per each treatment in one sequence. This regularly resulted in an extremely tedious task, that should only be considered for few well trained and extraordinary performing test subjects. Since, in the first instance, we intended to find effect sizes g for a rather untrained, non-preconditioned test panel, we set up playback for a mixed randomized sequence of all 125 trials, divided in 4 parts ($35 + 3 \cdot 30$) with longer intermissions. Thus, the results to be presented in the next section, should be considered for this conditioning.

3.5. Results

3.5.1. Tests on Binomial Distribution

The detection rates (correct discrimination between original and phase shifted version) of all test subjects for all treatments are shown as a scatter plot in Fig. 4. For the -90° phase shifted square wave burst, except of three subjects, all other perform with very high, statistically significant detection rates between 76% and 100%. For the -45° phase shifted square wave burst, except of the same three subjects, all other show very high, statistically significant detection rates between 80% and 100%.

The -90° phase shifted pink noise treatment exhibits only one result for which guessing can be excluded by statistical significance. This was produced by one of the preconditioned, trained authors. The majority of detection is slightly below guessing. About the same situation, however with larger spread of the rates, can be observed for the -90° phase shifted castanets treatment. The one statistically significant result was achieved by another trained, preconditioned author. All other detection rates fail to reject that guessing took place.

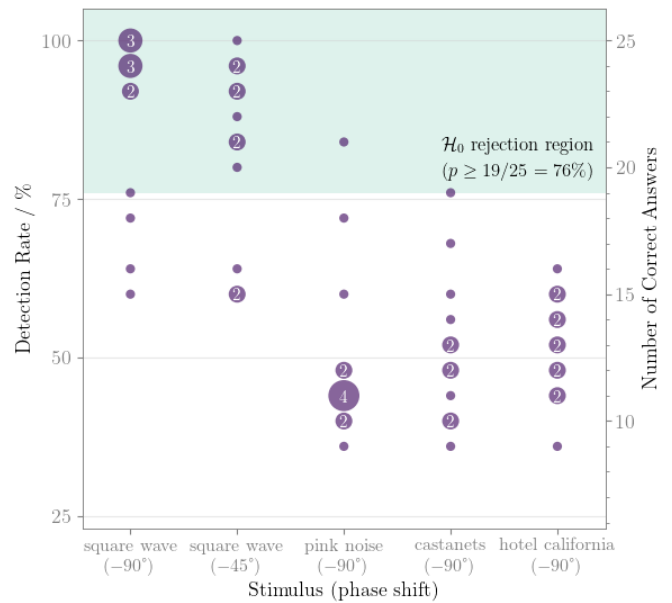


Fig. 4: Detection rates in percent and number of correct detections of all test panelists. Small dots without numbering indicate a performance of a single test subject, whereas increasing dots with numbering indicate same performance for multiple test subjects. Results within the shaded area indicate that guessing is unlikely with statistical significance.

For the musical content, i.e. the percussion sequence in Hotel California, no statistical significance can be reported. Detection rates spread around the guessing rate ranging from 36% to 64%.

3.5.2. Tests on Chi-Square Distribution

The \mathcal{H}_0 (correct and incorrect discrimination occur with equal frequency) is tested with the χ^2 test per treatment considering all judgments. Bonferroni correction for total of 5 treatments to a target $\alpha = 0.05$ was considered. The results indicate that this \mathcal{H}_0 can be rejected with very high statistical significance for the two square wave bursts, but not for the other three treatments.

The \mathcal{H}_0 (detection performance of two treatments is independent) is tested with the χ^2 test of the contingency table built from two treatments considering all judgments. Bonferroni correction for the 10 possible pairwise comparisons to a target $\alpha = 0.05$ was considered. The results indicate that this \mathcal{H}_0 can be rejected for the pairs I vs. III, IV, V and II vs. III, IV, V with very high statistical significance and odds ratios (ORs) between 4.5 to 6.5. For the pairs I vs. II and III vs. IV, V and IV vs. V we fail to reject this \mathcal{H}_0 . For pairwise comparison I vs. II the OR ≈ 1.4 indicates a very small (however statistically not significant, $p = 0.17$) tendency for a different performance. For the other pairs OR ≈ 1 indicates very comparable rating performance.

3.5.3. Rating Durations

Test subjects took between 70 and 120 minutes in total for the whole listening experiment, including intermissions. One test subject asked to split the test onto two days for improved power of concentration.

The webMUSHRA software captures data for rating durations of all trials. This duration is defined as the time interval from initiating the GUI for the actual trial up to submitting the result and moving on with the next trial. Thus, this duration measure includes all (potentially longer) individual intermissions of a test subject. Pure playback duration of A, B, X per trial, which is considered a more useful measure, is unfortunately not available. We thus report the percentiles in Table 1 over all rating durations t in seconds without further statistic evaluation. However, the table easily reveals that the median and the interquartile range—that should not overly affected by longer intermission intervals—increase following the treatment sequence I to V.

treatment	$t_{0.05}/s$	$t_{0.25}/s$	$t_{0.5}/s$	$t_{0.75}/s$	$t_{0.95}/s$
I sq -90	8.1	12.4	17.7	29.2	60.9
II sq -45	8.9	15.3	23.1	39.8	95.2
III pn -90	13.7	19.8	28.7	47.4	98.6
IV cas -90	11.5	20.2	30.0	48.2	109.7
V hc -90	12.6	24.4	35.9	52.5	104.2

Tab. 1: Percentiles of the rating duration per ABX trial.

3.5.4. Qualitative Statements

Test subjects were asked for handwritten qualitative statements (e.g. detection cues, artifacts) during the listening experiment. Since this was handled as unforced add-on not all panelists reported back. However, the received statements are highly valuable and can be summarized as follows.

Treatments using square wave bursts were comparably very easy to detect, and comparing both square waves, the -90° treatment was much easier to detect than the one with -45° . Most often pitch shifts were used as cues, but also changes in envelopment and dispersion were reported.

The detection of pink noise treatments was reported as very demanding. Here test subjects indicated changed pitch, roughness, sharpness, subbass structure, melody and ambience as cues. For castanets test subjects reported a hard time for detection and admitted pure guessing very often using either the pitch or/and the characteristics of the very first transient (change of attack, punch and crispness) to discriminate treatment and reference. No pre-/postringing artifacts were stated for the castanets.

For the percussion sequence (Hotel California) most reports agreed on pure guessing. However, test subjects also reported there to use changed decay of drumheads and changed pitch as cues as well as smeared transients.

One test subject reported that A,B and X were perceived with different pitches for the square wave bursts. Here, due to the forced choice design, the achieved detection rates must fail to reject \mathcal{H}_0 , which was confirmed post-hoc.

4. Conclusion

This study exhibits explorative character to firstly evaluate the audibility of constant phase shifts. For signals with rather complex structure, arbitrary constant phase shifts can only be realized with digital signal processing. Based on the Hilbert transform (i.e. the special case of -90° constant phase

shift with unit magnitude), for which the infinite impulse responses are well known in continuous-time and discrete-time signal domain, this paper introduces the discrete-time infinite impulse response for an arbitrary constant phase shifter. For practical implementations an FIR design is proposed with special attention to retain unit magnitude. Furthermore, for periodic signals a periodic convolution is discussed. Under the periodicity assumption, hereby the ideal phase shift filter without any approximations or limitations can be applied. The periodic convolution can be computed within DFT domain with high performance, for which the spectrum of the constant phase shifter is given.

The results of the conducted listening experiment can be referred to the following deductions. Untrained, unconditioned listeners that have been repeatedly confronted with multiple low frequency square wave bursts, lowpass filtered noise, a transient castanet rhythm and a percussion sequence in a randomized sequence, in general show different detection performances of applied constant phase shifts.

The majority of listeners was able to discriminate constant phase shifts of -90° and -45° for square wave bursts with comparably little demand and very high detection rate. A 100% detection rate was achieved by musical experts. These findings are according to the known results with respect to other low frequency group delay distortion of square waves.

For pink noise the majority of listeners is not able to detect constant phase shift treatments of -90° . However, the results indicate that by musical background and audio expertise higher detection rates can be achieved, that might be tested for statistical significance by a more sensitive test design. An adapted effect size of about $g = 0.2$ to 0.25 seems to be reasonable for this. The same observation and conclusion holds for the -90° constant phase shift of the castanets signal. For both signals trained listeners are able to detect the treatment with statistical significance. The initial guessed effect size can be well assumed for both stimuli.

All listeners were not able to detect constant phase shift of -90° for the sequence containing percussion material with full audio bandwidth. Here, highest judgment demand was reported by qualitative statements, very often admitting pure guessing. The comparably longest rating durations might reflect this fact as well. This insensitivity might be due to complex spectrum and full audio bandwidth, compared to the other used audio contents. An adapted effect size of about $g = 0.15$ seems to be an appropriate choice for a more sensitive test design (e.g. addressing significant detection rates $\frac{\geq 69 \text{ correct}}{119 \text{ total}}$ of single treatment judgment for $\alpha = \beta = 0.05$).

Although, here only shown in an ABX comparison scenario and not yet for musical contents, we cannot fully exclude that very critical, trained listeners are able to detect constant phase shifts of well known references even in a non-comparison task as well. Considering this circumstance and the current listening experiment results, it appears advisable to apply constant phase shift filters in 2.5D and 3D sound field synthesis applications to perfectly guarantee that potentially audible phase shift artifacts will not occur.

Open Science

This project is following the open science paradigm. Please find all relevant code and data in the related git repository⁴. The DOI <https://doi.org/10.5281/zenodo.3383286> is directly related to the repository's state when submitting the paper. The repository includes Jupyter notebooks for signal processing calculus and statistical evaluation, stand-alone Python code to create all presented figures, the tex source code for the paper and the related talk, the raw data from the listening experiment, the code modifications of the used ABX software as well as the ABX configuration files. Besides the copyrighted piece of music, all other audio content used for the listening experiment is freely available.

5. References

- [1] D. G. Meyer, "Digital control of loudspeaker array directivity," *J. Audio Eng. Soc.*, vol. 32, no. 10, pp. 747–754, 1984.
- [2] —, "Multiple-beam, electronically steered line-source arrays for sound-reinforcement applications," *J. Audio Eng. Soc.*, vol. 38, no. 4, pp. 237–249, 1990.
- [3] F. Schultz, "Sound field synthesis for line source array applications in large-scale sound reinforcement," Ph.D. dissertation, University of Rostock, 2016.
- [4] S. Spors, R. Rabenstein, and J. Ahrens, "The theory of wave field synthesis revisited," in *Proc. 124th Audio Eng. Soc. Conv.*, Amsterdam, 2008.
- [5] F. Zotter and S. Spors, "Is sound field control determined at all frequencies? How is it related to numerical acoustics?" in *Proc. 52nd Int. Conf. Audio Eng. Soc. (AES)*, 2013.
- [6] C.-C. Tseng, S.-C. Pei, and S.-C. Hsia, "Computation of fractional derivatives using Fourier transform and digital FIR differentiator," *Signal Processing*, vol. 80, no. 1, pp. 151–159, January 2000.
- [7] B. Krishna, "Studies on fractional order differentiators and integrators: A survey," *Signal Processing*, vol. 91, no. 3, pp. 386–426, March 2011.
- [8] S. Spors and J. Ahrens, "Analysis and improvement of pre-equalization in 2.5-dimensional wave field synthesis," in *Proc. 128th Audio Eng. Soc. Conv.*, London, 2010.
- [9] H. Wierstorf, "Perceptual assessment of sound field synthesis," Ph.D. dissertation, Technische Universität Berlin, 2014.
- [10] F. Winter, "Local sound field synthesis," Ph.D. dissertation, University of Rostock, 2019 (to be appear).
- [11] C. Salvador, "Wave field synthesis using fractional order systems and fractional delays," in *Proc. 128th Audio Eng. Soc. Conv.*, London, 2010.
- [12] F. Schultz, V. Erbes, S. Spors, and S. Weinzierl, "Derivation of IIR-pre-filters for soundfield synthesis using linear secondary source distributions," in *Proc. AIA-DAGA*, Meran, 2013.
- [13] V. Hansen and E. R. Madsen, "On aural phase detection," *J. Audio Eng. Soc.*, vol. 22, no. 1, pp. 10–14, January/February 1974.
- [14] —, "On aural phase detection: Part ii," *J. Audio Eng. Soc.*, vol. 22, no. 10, pp. 783–788, December 1974.
- [15] J. Blauert and P. Laws, "Group delay distortions in electroacoustical systems," *J. Acoust. Soc. Am.*, vol. 63, no. 5, pp. 1478–1483, 1978.
- [16] H. Suzuki, S. Morita, and T. Shindo, "On the perception of phase distortions," *J. Audio Eng. Soc.*, vol. 28, no. 9, pp. 570–574, September 1980.
- [17] S. P. Lipshitz, M. Pocock, and J. Vanderkooy, "On the audibility of midrange phase distortion in audio systems," *J. Audio Eng. Soc.*, vol. 30, no. 9, pp. 580–595, September 1982.
- [18] H. Møller, P. Minnaar, S. K. Olesen, F. Christensen, and J. Plogsties, "On the audibility of all-pass phase in electroacoustical transfer functions," *J. Audio Eng. Soc.*, vol. 55, no. 3, pp. 115–134, March 2007.
- [19] A. W. Lohmann, D. Mendlovic, and Z. Zalevsky, "Fractional Hilbert transform," *Opt. Lett.*, vol. 21, no. 4, pp. 281–283, 1996.
- [20] S. L. Hahn, *Hilbert Transforms in Signal Processing*. Boston: Artech House, 1996.
- [21] A. V. Oppenheim, R. W. Schaffer, and J. R. Buck, *Discrete-Time Signal Processing*. Upper Saddle River: Prentice Hall, 1999.
- [22] M. Abramowitz and I. A. Stegun, *Handbook of Mathematical Functions*. New York: Dover, 1970.
- [23] M. Schoeffler, S. Bartoschek, F.-R. Stöter, M. Roess, S. Westphal, B. Edler, and J. Herre, "webMUSHRA—a comprehensive framework for web-based listening tests," *J. Open Res. Softw.*, vol. 6, no. 1, p. 8, 2018.
- [24] Recommendation ITU-R BS.1770-4, "Algorithms to measure audio programme algorithms to measure audio programme loudness and true-peak audio level," ITU, Tech. Rep., 2017.
- [25] D. C. Howell, *Statistical Methods for Psychology*, 8th ed. Belmont: Wadsworth, Cengage Learning, 2013.
- [26] F. Faul, E. Erdfelder, A.-G. Lang, and A. Buchner, "G*Power 3: A flexible statistical power analysis program for the social, behavioral, and biomedical sciences," *Behavior Research Methods*, vol. 38, no. 2, pp. 175–191, 2007.

⁴ <https://github.com/spatialaudio/audibility-constant-phase>